1.E.1:
1.E.4

Nuclear Physics **A230** (1974) 285—301; © *North-Holland Publishing Co., Amsterdam*

STUDY OF ^{29}Al WITH THE ^{26}Mg(α, pγ)^{29}Al REACTION

P. EKSTRÖM† and J. TILLMAN†

Fysisch Laboratorium, Rijksuniversiteit, Utrecht, The Netherlands

Received 11 June 1974

Abstract: Particle-γ angular correlation and DSA measurements with the ^{26}Mg(α, pγ)^{29}Al reaction have been used to obtain spectroscopic information on ^{29}Al levels. Excitation energies, branching and mixing ratios and mean lifetimes have been determined for a number of levels up to 6 MeV excitation energy. The following new J^π assignments have been made: $J^\pi(2.22) = \frac{3}{2}^+$ and $J^\pi(3.18) = \frac{5}{2}^+$. In addition, several J^π limitations have been inferred. The experimental results are compared with shell model calculations.

E

NUCLEAR REACTIONS ^{26}Mg(α, pγ), E = 14.2, 16.5, 18.0 MeV; measured pγ(θ), γγ-coin, DSA, $\sigma(E_p, E_\gamma)$. ^{29}Al levels deduced E_x, τ_m, J, π, γ-branchings, mixing ratios, s. Enriched target.

1. Introduction

Although many nuclei in the 2s1d shell have been thoroughly studied, there remain several, the present knowledge of which is rather rudimentary. One such nucleus is ^{29}Al. When the present investigation was started only five unambiguous J^π assignments had been made for this nucleus [1]).

Charged particle angular distribution measurements have been reported with the ^{27}Al(t, p)^{29}Al [refs. [2,3])], ^{30}Si(d, τ)^{29}Al [ref. [4])] and ^{30}Si(t, α)^{29}Al [ref. [5])] reactions yielding excitation energies, spectroscopic factors and some J^π assignments and limitations. Particle-γ angular correlation measurements with NaI detectors with the ^{26}Mg(α, pγ)^{29}Al reaction [3,6]) and the ^{27}Al(t, pγ)^{29}Al and ^{30}Si(t, αγ)^{29}Al reactions [7]) have yielded the decay and spin limitations of some states. Recently, Beck *et al.* [8]) have determined excitation energies and mean lifetimes of some low-lying states. The ^{29}Mg(β^-)^{29}Al decay has been studied by Goosman *et al.* [9]).

Shell model calculations on ^{29}Al have been performed by De Voigt *et al.* [10,11]). Levels of ^{29}Al have been interpreted in terms of the Nilsson model by Hirko *et al.* [3]), Kean *et al.* [6]) and Jones *et al.* [12]).

The present investigation of p-γ angular correlations with the ^{26}Mg(α, pγ)^{29}Al reaction was performed to gain additional spectroscopic information on ^{29}Al. Gamma rays were detected with a Ge(Li) detector which, due to its superior energy resolution and in spite of its lower detection efficiency, yields results not obtainable with NaI detectors. In sect. 2 the experimental procedure is described. The results from the

† Permanent address: Department of Nuclear Physics, University of Lund, Lund, Sweden.

angular correlation and DSA measurements are given in sect. 3, and finally a comparison with the theory is given in sect. 4.

2. Experimental procedure and analysis

The experiment was performed with α-particles from the Utrecht 6 MV tandem Van de Graaff accelerator. The target chamber consisted of an Al cylinder 12 cm in diameter. A beam current in the range 100–300 nA was maintained on the target. A 3 mm Ta diaphragm restricted the size of the beam, which after passing through the target was stopped in a Faraday cup 5 m from the target.

The targets consisted of 50–100 $\mu g/cm^2$ ^{26}Mg enriched to 99.4 % and evaporated on 30 $\mu g/cm^2$ C foils. For the DSA lifetime measurements (see subsect. 2.2) Au backings were used.

A 2 mm thick annular surface-barrier Si counter detected protons between 163° and 173°. Elastically scattered α-particles were stopped in mylar foils (100 μm thick for C-backed targets) placed in front of the Si detector. Fig. 1 shows a spectrum of protons coincident with all γ-rays. The resolution is about 90 keV, mostly due to straggling in the mylar foil and reaction kinematics.

Gamma rays were detected with a Philips 25 % efficiency 125 cm^3 Ge(Li) detector, which had a resolution of 2.4 keV at 1.33 MeV. The detector subtended a half-angle of 12° at the target. Low-energy γ-rays were suppressed by a 3 mm thick Pb plate

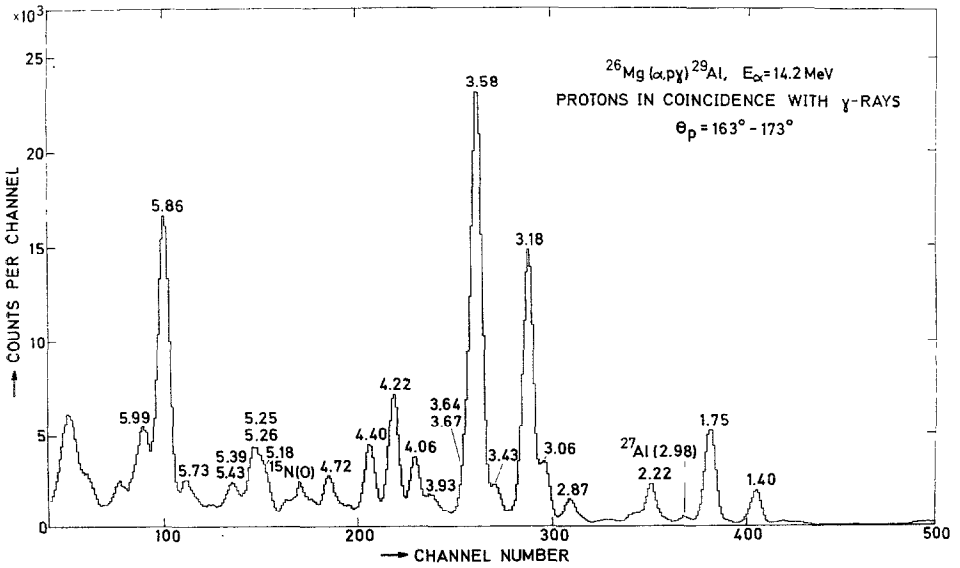

Fig. 1. Spectrum of protons coincident with γ-rays from the $^{26}Mg(\alpha, p\gamma)^{29}Al$ reaction at $E_\alpha = 14.2$ MeV. Random coincidences have been subtracted. The corresponding excitation energies (in MeV) in ^{29}Al are indicated. The peaks labelled $^{15}N(0)$ and $^{27}Al(2.98)$ result from the $^{12}C(\alpha, p)^{15}N$ and $^{24}Mg(\alpha, p)^{27}Al$ reactions, respectively.

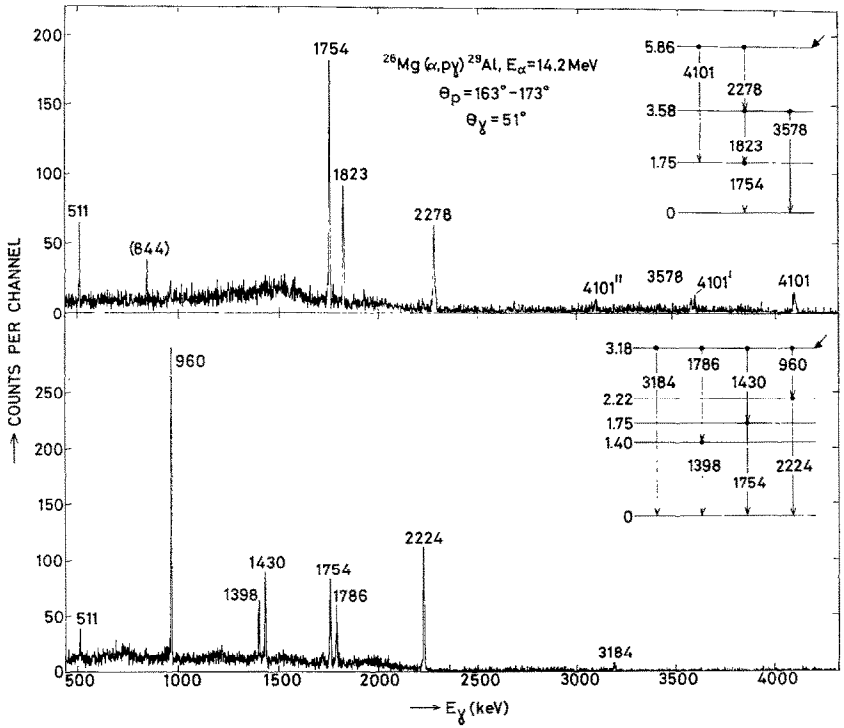

Fig. 2. Examples of γ-ray spectra at 51° in coincidence with proton groups corresponding to the levels indicated by arrows in the inserts. Random coincidences have not been subtracted. The peaks are marked with the transition energies (in keV) corrected for Doppler shift. The 511 keV peak results from positon annihilation and the 844 keV peak from the 0.84 → 0 MeV transition in ^{27}Al. Peaks marked with one or two primes are single or double escape peaks, respectively.

placed in front of the detector. Fig. 2 shows two γ-ray spectra coincident with different proton groups.

Coincidences between protons and γ-rays were detected with constant fraction timers and time-to-amplitude converters. The data were processed by a multi-parameter data acquisition system [13]), with event-mode recording on magnetic tape for later off-line sorting and analysis. The time spectra were Gaussian-shaped with FWHM of about 10 ns. The true-to-random coincidence ratio was usually so good (> 15) that random coincidences could be neglected.

A measurement of the yield of the different proton groups as a function of the bombarding energy E_α shows strong fluctuations. For $E_\alpha > 15$ MeV the overall yield decreases with increasing E_α. An energy $E_\alpha = 14.20$ MeV was used for most measurements since it gave optimum yield for many levels (see also, however, subsect. 2.2).

2.1. EXCITATION ENERGIES

Excitation energies have been determined from runs with the Ge(Li) detector at $\theta_\gamma = 90.0 \pm 0.5°$ relative to the beam. Sources of ^{228}Th, ^{88}Y, ^{60}Co and ^{56}Co were used for energy calibration [14]). The 6.13 → 0 MeV transition in ^{16}O resulting from the ^{16}O(α, α′)^{16}O reaction served as a high-energy calibration point [14]). Calibration γ-rays were recorded in coincidence in the Ge(Li) detector during the on-line measurements by the addition of a 12.7 cm × 12.7 cm NaI crystal, which was shielded from target γ-rays and from γ-rays scattered in the Ge(Li) detector itself. The p-γ and γ-γ coincidences were stored on magnetic tape together with labels indicating the detectors in coincidence. This procedure eliminated possible shifts in the Ge(Li) channel.

Peak positions were determined from first-moment calculations after subtraction of Compton tails from higher-energy γ-rays. Gamma-ray energies E_γ were calculated from a third-degree polynomial fitted to the calibration points. Level spacings were determined from the measured γ-ray energies by correction for the recoil of the ^{29}Al nucleus and for the transverse Doppler effect. The latter effect amounted to about 0.3 keV for $E_\gamma = 2$ MeV. The errors in the excitation energies were calculated as the

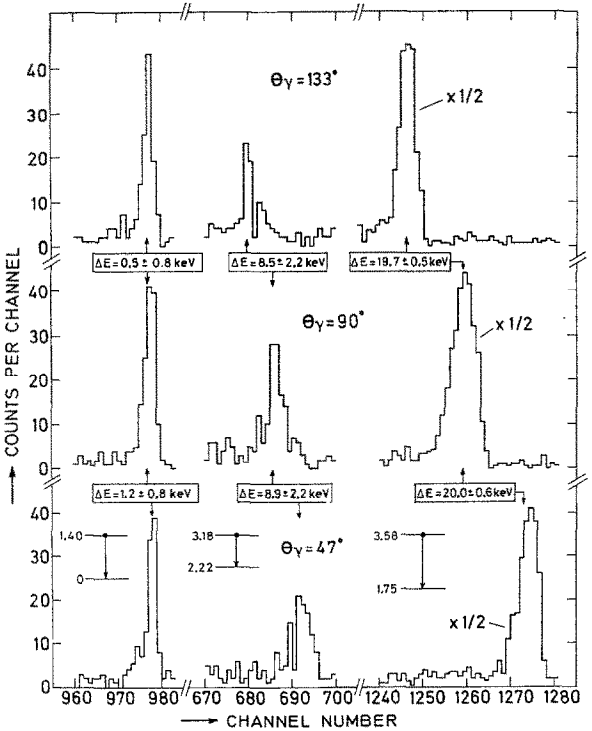

Fig. 3. Typical γ-ray Doppler shifts observed at $\theta_\gamma = 47°$, 90° and 133° in coincidence with protons from the reaction ^{26}Mg(α, pγ)^{29}Al.

quadratic sum of the contributions from the uncertainties in the peak positions, the uncertainties in the calibration energies and a possible 0.5° deviation of the Ge(Li) detector position from 90°.

2.2. LIFETIME MEASUREMENTS

For the lifetime measurements a target consisting of 90 μg/cm^2 ^{26}Mg evaporated on a 4.2 mg/cm^2 Au foil was placed perpendicular to the beam. Elastically scattered α-particles were stopped in a 250 μm mylar foil in front of the Si detector. Higher bombarding energies, E_α = 16.50 and 18.00 MeV, were used because protons corresponding to higher levels were stopped in the mylar foil at E_α = 14.2 MeV. Most data were taken from the E_α = 16.5 MeV run, but for some higher levels the E_α = 18.0 MeV run was used.

Data were taken in short (≈ 2 h) runs with the Ge(Li) detector at angles of 47.0°, 90.0° and 133.0° and at a distance of 13 cm from the target. During the lifetime measurements γ-rays from a ^{56}Co source were simultaneously recorded as described in subsect. 2.1. This served as a check on the stability of the γ-ray detection system and also as an energy calibration. No significant shifts were detected during three days of measurements.

Peak positions were determined as described in subsect. 2.1. Fig. 3 shows a few transitions at the three angles. It can be seen that the decay of the rather long-lived 1.40 MeV level shows very little shift, confirming that the backing was thick enough to stop the recoiling ^{29}Al nuclei.

The experimental attenuation factors $F(\tau_m)$ were determined from a least-squares fit to the expression

$$E = E_0\left\{1 + \frac{v(0)}{c} F(\tau_m)\cos\theta_\gamma\right\},$$

where E is the measured energy, E_0 the transition energy and $v(0)$ the initial recoil velocity of the final nucleus. The relative velocity $v(0)/c$ calculated from reaction kinematics took values in the range 1.65 to 1.75 %, depending on the excitation energy. The effect of the finite solid angle of the Si detector on the initial velocity was found to be negligible. Possible effects due to the finite solid angle of the Ge(Li) counter and to angular correlations, calculated for extreme conditions, were also found to be negligible.

Theoretical values of $F(\tau_m)$ were calculated as described by Engelbertink and Van Middelkoop [15]) with the theory of Lindhard *et al.* [16]) and the Blaugrund approximation [17]). The target was assumed to consist of four equally thick layers with identical yield. For the nuclear stopping power the theoretical estimate given by Lindhard *et al.* [16]) was used. The velocity dependence of the reduced electronic stopping power ξ_e [for a definition see ref. [15])] was expanded as

$$\xi_e = c_0 + c_1\frac{v}{c} + c_2\left(\frac{v}{c}\right)^2,$$

and the parameters c_i were determined from a fit to the values of the electronic stopping power S_e given by Northcliffe and Schilling [18]). For the target material the value of ξ_e for Al was used, since ξ_e does not depend strongly on the stopping medium.

The errors in the mean lives were calculated by quadratic addition of the statistical error in the experimental F-value and a 16 % error (the maximum value for the F-values measured) in the theoretical $F(\tau_m)$ curve. The latter error was comprised of a 10 % uncertainty in the density, a 10 % uncertainty in the stopping powers of the target and the backing material and a 25 % uncertainty in the target thickness. Since the initial recoil velocity was rather high, the relatively well-known electronic stopping power dominates over the nuclear stopping power and thus a 10 % uncertainty in total stopping power was taken as a reasonable estimate.

2.3. ANGULAR CORRELATION MEASUREMENTS

In the angular correlation measurements γ-rays were detected at $\theta_\gamma = 90.0°$, 63.4°, 50.8°, 39.2° and 26.6°. The Ge(Li) detector was placed 12 cm from the target. The angles were changed every 2 h in order to minimize possible systematic effects. Data were collected for a total of 16 h per position.

The efficiency of the γ-ray detection system in the range 0.8–3.5 MeV was measured for each angle with a ^{56}Co source. The uncertainty in the efficiency was estimated to be 5 %. The isotropy of the set-up was found to be so good that the same efficiency could be used for all five angles. The Doppler shift had a negligible effect on the efficiency.

For normalization purposes a random sample of the singles proton spectrum was continuously collected on magnetic tape by accepting random coincidences between protons and pulses from a 15 kHz pulser. The isotropic 1.40 → 0 MeV transition served as a check on the normalization.

Peak areas were calculated after subtraction of Compton tails from higher-energy γ-rays. The experimental correlations were fitted by a least-squares method to the Legendre polynomial expansion $W(\theta_\gamma) = A_0\{1+a_2P_2(\cos\theta_\gamma)+a_4P_4(\cos\theta_\gamma)\}$. The coefficients A_0, corrected for the γ-ray detection efficiency, were used for calculating the branching ratios. The errors in the branching ratios were calculated taking into account correlated errors.

The analysis of the angular correlations was carried out as described by Poletti and Warburton [19]). Theoretically the angular distribution from an aligned state with spin J_i decaying by γ-ray emission to a state with spin J_f is given by

$$W(\theta_\gamma) = \sum_{k \text{ even}} \rho_k(J_i)F_k(J_i, J_f, \delta)\mathcal{Q}_k P_k(\cos\theta_\gamma),$$

where ρ_k are statistical tensors which depend on the population parameters $p(m)$, F_k are angular distribution coefficients depending on the multipole mixing ratio

δ, Q_k are the γ-ray detector solid-angle attenuation coefficients and θ_γ is the γ-ray detection angle with respect to the quantization axis, in this case the beam direction. In the present experiment the geometry of method II of Litherland and Ferguson [20]) was used, and ideally only the lowest magnetic substates $m = \pm\frac{1}{2}$ were populated. Due to the finite size of the Si detector the $m = \pm\frac{3}{2}$ substates could be populated to a small extent [20]). It was checked that a 10 % population of the higher substates did in no case significantly change the results of the analysis. For the attenuation coefficients the values $Q_2 = 0.97$ and $Q_4 = 0.91$, calculated with the program of Krane [21,22]), were used.

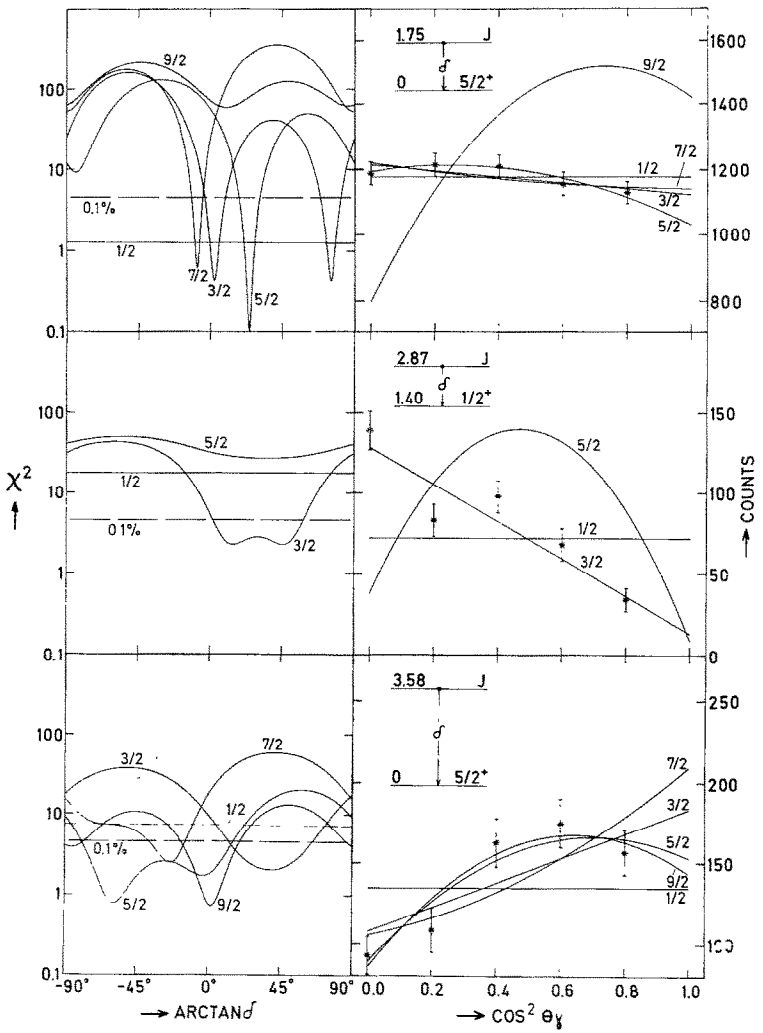

Fig. 4. Angular correlation data with theoretical fits and the corresponding χ^2 curves for the 1.75 → 0, 2.87 → 1.40 and 3.58 → 0 MeV transitions.

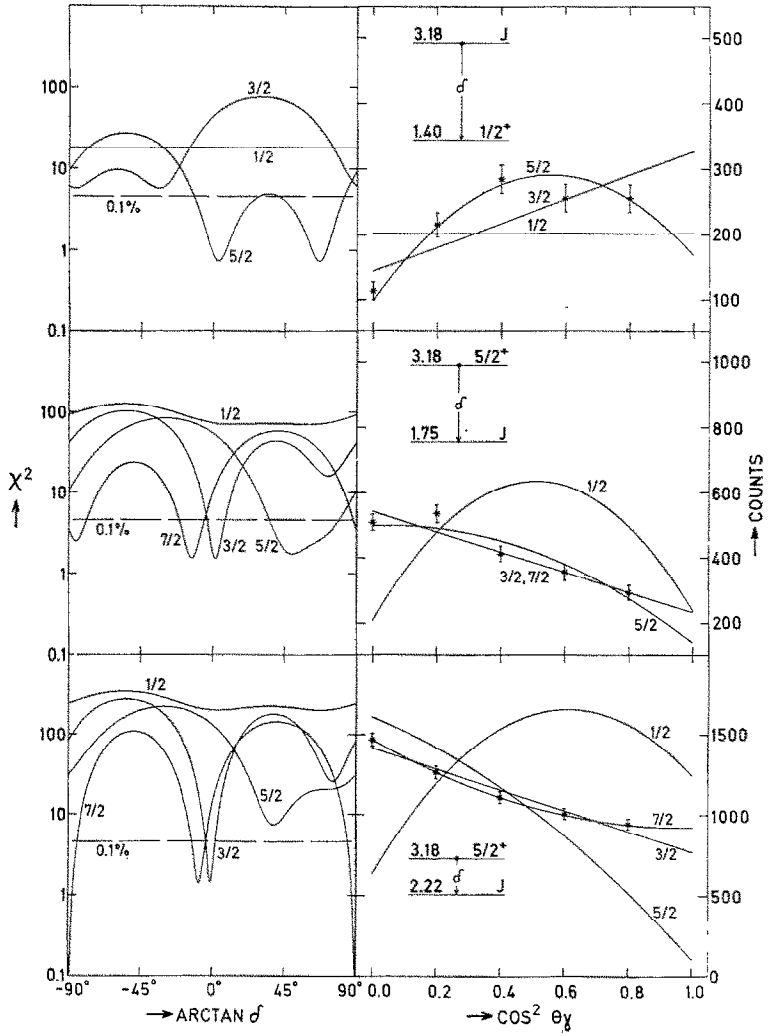

Fig. 5. Angular correlation data with theoretical fits and the corresponding χ^2 curves for the 3.18 → 1.40, 3.18 → 1.75 and 3.18 → 2.22 MeV transitions.

For each possible combination of J_i and J_f and for different values of the mixing ratio δ the best fit (one free parameter: the normalization A_0) and the goodness of fit χ^2 were calculated. The sign convention of Rose and Brink [23]) was used for the mixing ratio. The values of arctan δ were varied in steps of 1° (or smaller steps when necessary for determining the best value of arctan δ) from $-90°$ to 90°. For spin restrictions the 0.1 % probability criterion was applied. Examples of angular correlations with the best theoretical fits and the corresponding χ^2 curves are shown in figs. 4 and 5. Possible J^π values were rejected if they yielded unacceptable transition strengths Γ_γ/Γ_W where Γ_W is the relevant Weisskopf estimate. The criteria of Endt

TABLE 1

Excitation energies (in keV) for ^{29}Al states

Present work	Other work		
	[a])	[b])	[c])
1398.2±0.3	1405±10	1397.7±0.4	1397.6±0.4
1754.5±0.3	1759± 6	1753.8±0.4	1753.7±0.4
2223.9±0.4	2228± 6	2223.8±0.4	2224.5±0.6
2865.7±0.6	2873± 6		2865.4±0.8
3062.0±0.5	3069± 6		3060.8±0.7
3184.4±0.5	3193± 6	3184.0±0.6	3185.0±0.8
3433.1±0.7	3439±10		
3577.8±0.6	3584± 8		3577.3±1.5
3641.3±0.9	3647±10		
3672.2±1.3	3679±10		
3934.6±1.4	3947±10		
3985 ±2	3993		
4056.8±0.7	4064		
4219.8±0.7	4228		
4403.3±1.0	4411		
4715.2±1.4	(4716)		
4828.9±1.3	(4846)		
4940.8±1.0	(4939)		
5023 ±3	(5024)		
5181 ±2	5190		
5248.3±1.7			
5263 ±3	5267		
5392 ±3	5395		
5433 ±4	(5424)		
5733 ±4	(5732)		
5855.5±1.0	(5869)		
5993.6±1.0	6002		

[a]) Ref. [1]); the brackets indicate excitation energies which do not follow the systematic trend (see subsect. 3.1).

[b]) From the ^{29}Mg($\beta^-\gamma$)^{29}Al reaction [9]).

[c]) From the ^{26}Mg(α, pγ)^{29}Al and ^{27}Al(t, pγ)^{29}Al reactions [8]).

and Van der Leun [24]) were used: if Γ_γ/Γ_W minus its error exceeded 100 W.u. for E2 and E3, 3 W.u. for M2 and 10 W.u. for M3 the solution was rejected. The limiting strengths given in the discussion in subsect. 3.4 are the calculated strengths minus the error determined from compounding errors in the mean lifetimes, branching ratios and mixing ratios. The errors in the mixing ratios were calculated by the method described in ref. [25]) with the correction of ref. [26]).

Only primary transitions were considered in the analysis, since the near-isotropy of transitions between low-lying states eliminated the possibility of obtaining information from secondary transitions.

3. Results

3.1. EXCITATION ENERGIES

The ^{29}Al excitation energies determined in the present investigation are collected in table 1 together with those from a recent compilation [1]) and from some more recent publications [8, 9]). For most levels there is a systematic difference in energy between the present results and those of the compilation. The bracketed entries, however, do not follow this systematic trend, and the level correspondence is thus uncertain. The results of the present work can be seen to be in good agreement with those of Goosman *et al.* [9]) and Beck *et al.* [8]).

3.2. MEAN LIFETIMES

The measured attenuation factors F and mean lifetimes τ_m are given in table 2. When the measured F-value differs from unity by less than one standard deviation an upper lifetime limit of two standard deviations is given. The lifetime limit of the

TABLE 2
Mean lifetimes from DSA measurements

E_x (MeV)	$F(\tau_m)$	τ_m(fs)				
		present work	[a])	[b])	[c])	average
1.40	0.05±0.03	5000^{+7000}_{-2000}	6500±500[d])		3300^{+2200}_{-1000}	6500±500
1.75	0.96±0.02	25±11	80±40	60±30	< 50	32±12
2.22	0.80±0.03	110±30	110±50	90±70	< 80	110±30
2.87	0.77±0.04	120±30		70±40	< 150	100±30
3.06	0.97±0.14	< 160	90±50	80±40	< 50	80±30
3.18	0.76±0.07	120±50	280±70	180±70	210±100	180±40
3.43		< 10 ns[e])				
3.58	0.94±0.02	36±10	< 70			
3.64	1.03±0.10	< 100				
3.67	1.01±0.10	< 100				
3.93	0.75±0.03	130±30				
3.99	1.00±0.04	< 40				
4.06	0.77±0.12	120±70				
4.22	0.90±0.04	60±20				
4.40	0.88±0.06	60±30				
4.83	0.88±0.05	60±30				
4.94	0.93±0.02	42±12				
5.02	0.92±0.08	< 120				
5.25	0.96±0.10	< 130				
5.26	0.78±0.13	110±70				
5.86	0.93±0.04	42±19				
5.99	1.02±0.10	< 90				

[a]) From the ^{26}Mg(α, pγ)^{29}Al reaction, DSA[8]).
[b]) From the ^{27}Al(t, pγ)^{29}Al reaction, DSA[8]).
[c]) From the ^{27}Al(t, pγ)^{29}Al reaction, DSA[12]).
[d]) From the ^{26}Mg(α, pγ)^{29}Al reaction, recoil distance [8]).
[e]) See text, subsect. 3.2.

3.43 MeV level was deduced from a comparison of spectra with gates on and close to the peak in the time spectrum. Table 2 also shows previous measurements of mean lifetimes of some low-lying levels. It can be seen that where a comparison is possible the present results are consistent with those previously obtained.

3.3. BRANCHING RATIOS

The decay scheme and branching ratios inferred from the present work are given in fig. 6. Upper limits of two standard deviations have been given for very weak and unobserved transitions. The branching ratios from the present work compare well with those given in refs. [3, 7]) with two exceptions. The $(14 \pm 1)\%$ branch depopulating

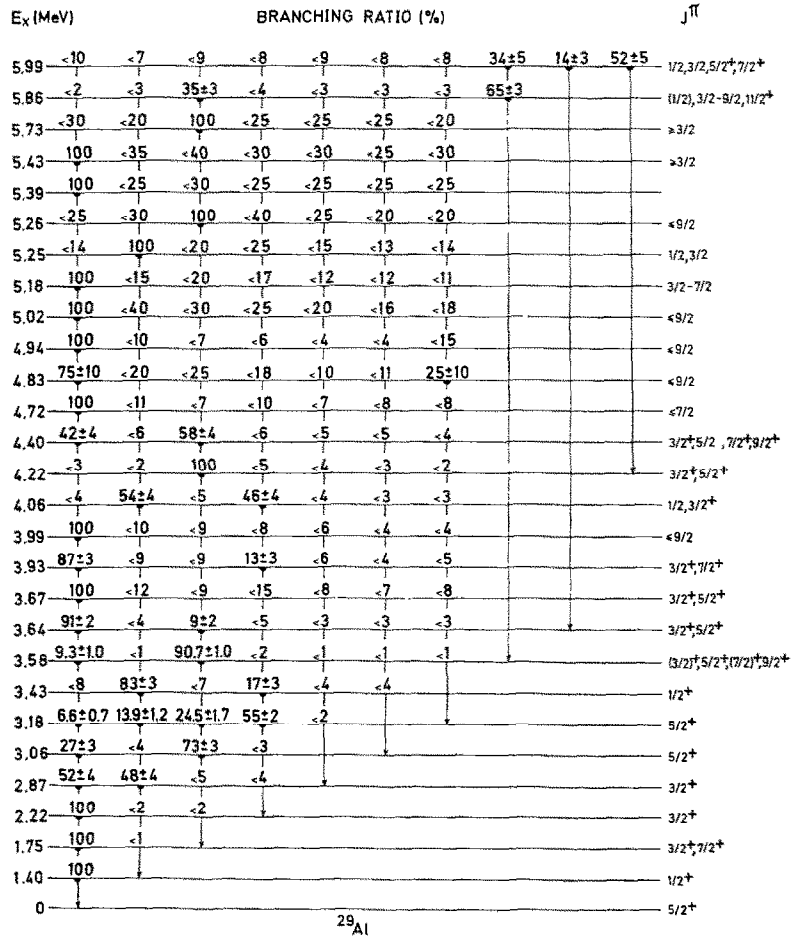

Fig. 6. The ^{29}Al level scheme and branching ratios from the present experiment. The J^{π} assignments are from the present work combined with previous data; see discussion in subsect. 3.4.

the 3.18 MeV level to the 1.40 MeV level (see fig. 2) was not observed by Jones *et al.* [7]). The 3.64 → 0 MeV branch is (91±2)% from the present work, whereas Jones *et al.* [7]) quote (56±3)%. In both cases the present results are in good agreement with the work of Hirko *et al.* [3]). The disagreement with the work of Jones *et al.* [7]) could be due to their use of a NaI detector.

3.4. J^π ASSIGNMENTS AND MULTIPOLE MIXING RATIOS

The Legendre polynomial expansion coefficients of the angular correlation of primary transitions are shown in table 3. Only the statistically significant a_4 coefficients are listed.

Some multipole mixing ratios δ are collected in table 4. Two criteria were used for selecting the mixing ratios given. Only those hypotheses giving distinct minima in the χ^2 *versus* arctan δ plot with more than 0.1 % confidence were accepted. Since the assignments $J^\pi(1.75) = \frac{7}{2}^+$ and $J^\pi(3.58) = \frac{9}{2}^+$ are considered to be very likely (see subsect. 4.1) only values consistent with these assumptions are included. The agreement with previously published [3, 6, 7]) values is good.

TABLE 3

Legendre polynomial expansion coefficients[a]) of the angular correlations of primary transitions

E_i (MeV)	E_f (MeV)	a_2[b])	E_i (MeV)	E_f (MeV)	a_2[b])
1.40	0	0.00±0.05	4.22	1.75	−0.11±0.05
1.75	0	−0.05±0.03	4.40	0	0.66±0.13
2.22	0	0.06±0.06		1.75	0.39±0.11
2.87	0	−0.52±0.13	4.72	0	0.09±0.12
	1.40	−0.83±0.09	5.18	0	−0.53±0.10
3.06	0	−0.27±0.14	5.25	1.40	−0.12±0.15
	1.75	−0.24±0.07	5.26	1.75	−0.8 ±0.2
3.18	0	0.63±0.14	5.39	0	−0.1 ±0.2
	1.40	0.44±0.09[c])	5.43	0	1.0 ±0.3
	1.75	−0.46±0.06	5.73	1.75	1.0 ±0.2
	2.22	−0.34±0.03[d])	5.86	1.75	0.30±0.10
3.43	1.40	−0.03±0.11		3.58	−0.15±0.05
3.58	0	0.43±0.12[e])	5 99	3.58	−0.21±0.17
	1.75	−0.13±0.02		4.22	−0.06±0.12
3.64	0	0.33±0.09			
3.67	0	0.09±0.12			
3.93	0	−0.76±0.12			
4.06	1.40	−0.19±0.12			
	2.22	−0.15±0.12			

[a]) Not corrected for the finite solid angle of the Ge(Li) detector.

[b]) The a_4 coefficients are given (as footnotes) only in those cases, in which their values are at least twice their standard deviations, and then a_2 corresponds to the fit with both a_2 and a_4.

[c]) $a_4 = -0.60 \pm 0.13$.

[d]) $a_4 = 0.11 \pm 0.05$.

[e]) $a_4 = -0.32 \pm 0.16$.

TABLE 4

Multipole mixing ratios, δ, for some transitions and assumed J^π values

E_i (MeV)	E_f (MeV)	J_i^π	J_f^π	δ[a])
1.75	0	$(\frac{7}{2}^+)$[b])	$\frac{5}{2}^+$	-0.147 ± 0.016
2.22	0	$\frac{3}{2}^+$	$\frac{5}{2}^+$	0.15 ± 0.04 or 2.7 ± 0.3
3.06	1.75	$\frac{5}{2}^+$	$(\frac{7}{2}^+)$[b])	-0.08 ± 0.04 or $\lvert\delta\rvert > 7$
3.18	1.40	$\frac{5}{2}^+$	$\frac{1}{2}^+$	0.07 ± 0.08
	1.75		$(\frac{7}{2}^+)$[b])	-0.23 ± 0.07 or $\lvert\delta\rvert > 6$
	2.22		$\frac{3}{2}^+$	-0.02 ± 0.02
3.58	0	$(\frac{9}{2}^+)$[c])	$\frac{5}{2}^+$	0.03 ± 0.09
	1.75		$(\frac{7}{2}^+)$[b])	-0.097 ± 0.014
3.64	0	$(\frac{5}{2}^+)$[b])	$\frac{5}{2}^+$	0.10 ± 0.08 or -2.3 ± 0.9
3.93	0	$(\frac{7}{2}^+)$[b])	$\frac{5}{2}^+$	0.23 ± 0.09 or 2.2 ± 0.6
4.06	1.40	$(\frac{3}{2}^+)$[d])	$\frac{1}{2}^+$	-0.16 ± 0.06 or 2.6 ± 0.5
	2.22		$\frac{3}{2}^+$	0.37 ± 0.10 or $\lvert\delta\rvert > 4$
4.22	1.75	$(\frac{5}{2}^+)$[b])	$(\frac{7}{2}^+)$[b])	0.02 ± 0.02 or 6.0 ± 1.0
5.25	1.40	$(\frac{3}{2})$[d])	$\frac{1}{2}^+$	-0.20 ± 0.08 or 3.0 ± 0.8
5.86	1.75	$(\frac{11}{2}^+)$[e])	$(\frac{7}{2}^+)$[b])	0.03 ± 0.10
	3.58		$(\frac{9}{2}^+)$[c])	-0.08 ± 0.03
5.99	3.58	$(\frac{7}{2}^+)$[f])	$(\frac{9}{2}^+)$[c])	-0.02 ± 0.12 or $\lvert\delta\rvert > 3$
	4.22		$(\frac{5}{2}^+)$[b])	-0.14 ± 0.04 or $\lvert\delta\rvert > 13$

[a]) The sign convention used is that of Rose and Brink [23]).
[b]) Also possible $J^\pi = \frac{3}{2}^+$.
[c]) Also possible $J^\pi = (\frac{3}{2}-\frac{7}{2})^+$.
[d]) Also possible $J = \frac{1}{2}$.
[e]) Also possible $J = \frac{1}{2}-\frac{9}{2}$.
[f]) Also possible $J^\pi = \frac{1}{2}, \frac{3}{2}, \frac{5}{2}^+$.

The J^π assignments and limitations from the present and other work [1]) are discussed below and summarized in fig. 6. Bracketed assignments have between 0.1 % and 10 % probability. The limiting strengths have been calculated from the averaged mean lifetimes in table 2.

3.4.1. New spin and parity assignments. The χ^2 analysis of the angular correlation of the 2.22 → 0 MeV transition excludes $J(2.22) > \frac{7}{2}$. In addition $J^\pi(2.22) = \frac{3}{2}^-$ is excluded since this would give an M2 strength of at least 7 W.u. The angular correlation of the strong 3.18 → 2.22 MeV transition (see fig. 5), together with the assignment $J^\pi(3.18) = \frac{5}{2}^+$ (see below), excludes $J(2.22) = \frac{1}{2}$ and $\frac{5}{2}$. The $(17\pm3)\%$ branch from the $J^\pi(3.43) = \frac{1}{2}^+$ level with a lifetime upper limit of 10 ns would give E3 or M3 strengths of more than 130 or 4000 W.u., respectively, for the 3.43 → 2.22 MeV transition if $J(2.22)$ were $\frac{7}{2}$. Conclusion: $J^\pi(2.22) = \frac{3}{2}^+$.

The lifetime of the 3.18 MeV level excludes decay by octupole transitions. The χ^2 analysis of the angular correlation of the 3.18 → 1.40 MeV transition only allows $J(3.18) = \frac{5}{2}$ (see fig. 5). Negative parity would give an M2 strength of at least 150 W.u., and thus $J^\pi(3.18) = \frac{5}{2}^+$.

3.4.2. Confirmed spin and parity assignment. The χ^2 analysis of the angular correlation of the 2.87 → 1.40 MeV transition (see fig. 4) excludes $\frac{1}{2}$ and $\frac{5}{2}$ as possible spins of the 2.87 MeV level. The assumption $J(2.87) = \frac{7}{2}$ would give an E3 strength of at least 8×10^6 W.u. or an M3 strength of more than 3×10^8 W.u. The assumption $J^\pi(2.87) = \frac{3}{2}^-$ would give an M2 strength of at least 20 W.u. The only remaining possibility $J^\pi(2.87) = \frac{3}{2}^+$ is in agreement with the previous [1]) assignment.

3.4.3. New spin limitations and parity assignments. The angular correlation of the 1.75 → 0 MeV transition (see fig. 4) gives the restriction $J(1.75) \leqq \frac{7}{2}$. From the lifetime and mixing ratio one can further exclude $\frac{7}{2}^-$, since this would give an improbably large M2 strength. The angular correlation of the 3.06 → 1.75 MeV transition excludes $J(1.75) = \frac{1}{2}$ and $\frac{5}{2}$. Since the 3.58 MeV level is known [1]) to have even parity, the admixture of a higher multipole in the 3.58 → 1.75 MeV transition excludes $J^\pi(1.75) = \frac{3}{2}^-$. Conclusion: $J^\pi(1.75) = \frac{3}{2}^+$ or $\frac{7}{2}^+$.

The 3.58 MeV level has positive parity [1]) and together with the correlation of the ground-state transition (see fig. 4) this yields the possibilities $J^\pi(3.58) = (\frac{3}{2})^+$, $\frac{5}{2}^+$, $(\frac{7}{2})^+$ or $\frac{9}{2}^+$, where the brackets indicate solutions with less than 10 % probability.

The 4.22 MeV level is known [1]) to have $J^\pi = \frac{3}{2}^+$ or $\frac{5}{2}^+$. If $J^\pi(1.75) = \frac{7}{2}^+$, then $J^\pi(4.22) = \frac{5}{2}^+$, since $\frac{3}{2}^+$ would require an improbably strong M3 component in the 4.22 → 1.75 MeV transition. The assumption $J^\pi(3.58) = \frac{9}{2}^+$ leads to the same assignment (see discussion of the 5.99 MeV level below), ensuring consistency for the proposed (see subsect. 4.1) ground-state rotational band.

An indication that the 5.86 MeV level has a rather high spin is that at high bombarding energies ($E_\alpha \approx 18$ MeV) the 5.86 MeV level is by far the strongest populated state. If it is assumed that $J(5.86) = \frac{11}{2}$, the assignment $J(3.58) = \frac{9}{2}$ follows from the angular correlation, and from this one can deduce $J(1.75) = \frac{7}{2}$.

The short lifetime of the 5.99 MeV level excludes decay by octupole transitions. The 5.99 → 4.22 MeV transition gives the limitation $J^\pi(5.99) = \frac{1}{2}, \frac{3}{2}, \frac{5}{2}^+$ or $\frac{7}{2}^+$, with the $\frac{7}{2} \rightarrow \frac{3}{2}$ hypothesis excluded. The assumption $J(3.58) = \frac{9}{2}$ requires $J^\pi(5.99) = \frac{7}{2}^+$.

The remaining limitations given in fig. 6 have been deduced by similar arguments.

4. Summary and discussion

The excitation energies of 27 levels up to $E_x = 6$ MeV have been determined (table 1) more accurately than before and at least one hitherto unobserved level has been found. Decay properties and mean lifetimes have been determined (fig. 6 and table 2) for many levels. Previous knowledge of these properties was rather scarce, especially for levels above $E_x = 3.58$ MeV. From this and previous work some unambiguous J^π assignment can be made (fig. 6), and some multipole mixing ratios have been inferred (table 4).

4.1. GROUND-STATE ROTATIONAL BAND

From the collective model one can infer that the odd (13th) proton is in Nilsson orbit 5 and that the deformation is prolate, since the ground state of ^{29}Al has $J^\pi =$

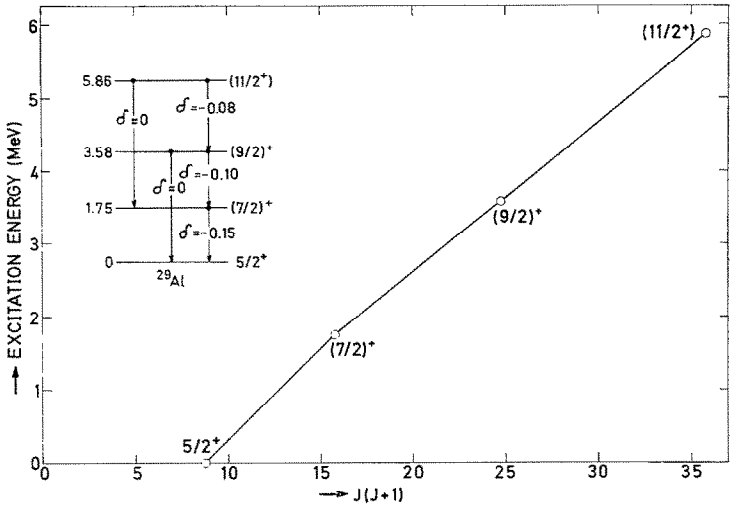

Fig. 7. Excitation energy *versus* $J(J+1)$ for the suggested ground-state rotational band shown in the insert.

$\frac{5}{2}^+$. It has been suggested [6, 12]) that the 1.75 and 3.58 MeV levels are the second and third $K^\pi = \frac{5}{2}^+$ levels built on the ground state. The decay of the 5.86 MeV level suggests that it might be the fourth member of this band. For a rotator with a constant moment of inertia the excitation energies are expected to follow the $J(J+1)$ rule, and one can see from fig. 7 that the levels mentioned follow this rule very closely.

The sign of the mixing ratio [sign convention from Rose and Brink [23])] for E2/M1 transitions within a rotational band is given by [27])

$$\text{sign}\,[\delta(\text{E2/M1})] = -\text{sign}\,[(g_K - g_R)/Q_0],$$

where g_K and g_R are the intrinsic and rotational g-factors, respectively, and Q_0 is the intrinsic quadrupole moment. For a proton in orbit 5, $g_K = 1.92$ [ref. [28])]. For g_R the estimate $g_R \approx Z/A = 0.45$ [ref. [28])] can be used, and Q_0 is positive for prolate deformation. Thus the sign of δ should be negative and this is in agreement with the experimental result for the 5.86 → 3.58, 3.58 → 1.75 and 1.75 → 0 MeV transitions (table 4).

4.2. COMPARISON WITH SHELL MODEL CALCULATIONS

If one makes the plausible assumption $J(1.75) = \frac{7}{2}$ (see subsect. 4.1), the spin and parity of the lowest eight levels are known and a comparison with theory could be meaningful (see fig. 8). The theoretical data have been calculated from the wave functions of De Voigt *et al.* [10, 29]) who performed a shell model calculation in a truncated $1d_{\frac{5}{2}}\,2s_{\frac{1}{2}}\,1d_{\frac{3}{2}}$ configuration space, with the modified surface delta interaction (MSDI) as an effective two-body interaction.

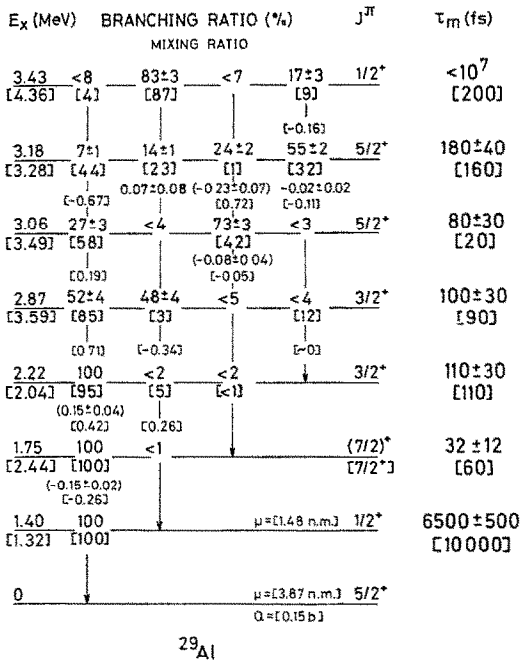

Fig. 8. Comparison of calculated [10]) (see subsect. 4.2) and measured quantities for ^{29}Al. The experimental data are from the present work except for the lifetimes, which are the averages given in table 2. Round brackets indicate incompletely determined experimental quantities, square brackets indicate theoretical data.

We have re-interpreted these theoretical results for ^{29}Al with the following modifications. The lowest $\frac{7}{2}^+$ and $\frac{3}{2}^+$ levels were identified with the 1.75 and 2.22 MeV states, respectively. The second $\frac{5}{2}^+$ level was identified with the 3.18 MeV state, and the third $\frac{5}{2}^+$ level [calculated but not mentioned in ref. [10])] with the 3.06 MeV state.

From the wave functions calculated by De Voigt *et al.* [29]) and the experimental excitation energies we calculated the multipole mixing ratios, lifetimes and branching ratios shown in square brackets in fig. 8. For the reduced single-particle matrix elements we used the bare-nucleon values instead of the two fitted effective matrix elements used in ref. [10]). As can be seen the agreement with experiment is good except for the excitation energies and a few transition strengths. It should be noted that this results from fitting only eight parameters [three single-particle energies, the four MSDI parameters and the isoscalar effective charge (e_p+e_n)] to known properties of $A = 27$–29 nuclei.

The problem of inconsistent spectroscopic factors for proton pick-up mentioned in a later paper by De Voigt and Wildenthal [11]) is resolved by our suggested interchange of the two upper $J^\pi = \frac{5}{2}^+$ levels mentioned above. The theoretical spectro-

scopic factors are 0.90 and 0.18 in fair agreement with the experimental values 1.76 and 0.10, respectively, obtained with the ^{30}Si(t, α)^{29}Al reaction [5,12]).

It is a pleasure to thank all at the Robert Van de Graaff Laboratory for their hospitality and willingness to help, and especially Prof. P. M. Endt and Prof. A. M. Hoogenboom for their kind interest and for putting excellent experimental facilities at our disposal. We also want to thank Dr. G. van Middelkoop for valuable help and reading the manuscript, Dr. P. W. M. Glaudemans for discussions concerning the theoretical calculations, Dr. H. A. Doubt for revising the English, F. E. H. van Eijkern and W. A. Sterrenburg for discussions and assistance. We gratefully acknowledge the financial assistance from the "Ministerie van Onderwijs en Wetenschappen" based on the Cultural Agreement Netherlands – Sweden.

References

1) P. M. Endt and C. van der Leun, Nucl. Phys. **A214** (1973) 1
2) A. A. Jaffe *et al.*, Proc. Phys. Soc. **76** (1960) 914
3) R. G. Hirko *et al.*, Particles and Nuclei **1** (1971) 372
4) R. C. Bearse, D. H. Youngblood and J. L. Yntema, Phys. Rev. **167** (1968) 1043
5) A. D. W. Jones, Phys. Rev. **180** (1969) 997
6) D. C. Kean, K. W. Carter, C. J. Piluso and R. H. Spear, Nucl. Phys. **A132** (1969) 241
7) A. D. W. Jones, J. A. Becker and R. E. McDonald, Phys. Rev. **187** (1969) 1388
8) F. A. Beck, T. Byrski, G. Costa and P. Engelstein, Nucl. Phys. **A218** (1974) 213
9) D. R. Goosman, C. N. Davids and D. E. Alburger, Phys. Rev. **C8** (1973) 1331
10) M. J. A. de Voigt, P. W. M. Glaudemans, J. de Boer and B. H. Wildenthal, Nucl. Phys. **A186** (1972) 365
11) M. J. A. de Voigt and B. H. Wildenthal, Nucl. Phys. **A206** (1973) 305
12) A. D. W. Jones, J. A. Becker and R. E. McDonald, Phys. Rev. **C3** (1971) 724
13) P. B. J. van Elswijk, R. Engmann, A. M. Hoogenboom and P. de Wit, Nucl. Instr. **96** (1971) 35
14) J. B. Marion, Nucl. Data **A4** (1968) 301
15) G. A. P. Engelbertink and G. van Middelkoop, Nucl. Phys. **A138** (1969) 588
16) J. Lindhard, M. Scharff and H. E. Schiøtt, Mat. Fys. Medd. Dan. Vid. Selsk. **33** (1963) no. 14
17) A. E. Blaugrund, Nucl. Phys. **88** (1966) 501
18) L. C. Northcliffe and R. F. Schilling, Nucl. Data Tables **A7** (1970) 233
19) A. R. Poletti and E. K. Warburton, Phys. Rev. **137** (1965) B595
20) A. E. Litherland and A. J. Ferguson, Can. J. Phys. **39** (1961) 788
21) K. S. Krane, Nucl. Instr. **98** (1972) 205
22) K. S. Krane, Nucl. Instr. **109** (1973) 401
23) H. J. Rose and D. M. Brink, Rev. Mod. Phys. **39** (1967) 306
24) P. M. Endt and C. van der Leun, At. Data and Nucl. Data Tables **13** (1974) 67
25) D. Cline and P. M. S. Lesser, Nucl. Instr. **82** (1970) 291
26) P. M. S. Lesser, D. Cline, P. Goode and R. N. Horoshko, Nucl. Phys. **A190** (1972) 597
27) E. K. Warburton, A. R. Poletti and J. W. Olness, Phys. Rev. **168** (1968) 1232
28) S. G. Nilsson, Mat. Fys. Medd. Dan. Vid. Selsk. **29** (1955) no. 16
29) M. J. A. de Voigt, P. W. M. Glaudemans, J. de Boer and B. H. Wildenthal, Utrecht University, private communication